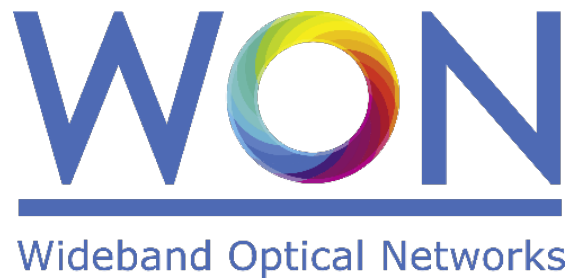


Marie Skłodowska-Curie (MSCA) – Innovative Training Networks (ITN)
H2020-MSCA-ITN European Training Networks



Wideband Optical Networks [WON]

Grant agreement ID: 814276

WP1: Network Management: Planning and Control
Deliverable D1.1: Wideband Fiber Transmission Modelling



This project has received funding from the European Union's Horizon 2020 research and innovation programme under the Marie Skłodowska-Curie grant agreement 814276.

Document Details

| | |
|-----------------------|---|
| Work Package | WP1: Network Management: Planning and Control |
| Deliverable number | D1.1 |
| Deliverable Title | Wideband Fiber Transmission Modelling |
| Lead Beneficiary: | Politecnico di Torino |
| Deliverable due date: | 30/06/2020 |
| Actual delivery date: | 08/01/2021 |
| Dissemination level: | Public |

Project Details

| | |
|----------------------|---|
| Project Acronym | WON |
| Project Title | Wideband Optical Networks |
| Call Identifier | H2020-MSCA-2018 Innovative Training Networks |
| Coordinated by | Aston University, UK |
| Start of the Project | 1 January 2019 |
| Project Duration | 48 months |
| WON website: | https://won.astonphotonics.uk/ |
| CORDIS Link | https://cordis.europa.eu/project/rcn/218205/en |

WON Consortium and Acronyms

| Consortium member | Legal Entity Short Name |
|--|-------------------------|
| Infinera Germany | INF G |
| Aston University | Aston |
| Danmarks Tekniske Universitet | DTU |
| VPIphotonics GmbH | VPI |
| Infinera Portugal | INF PT |
| Fraunhofer HHI | HHI |
| Politecnico di Torino | POLITO |
| Technische Universiteit Eindhoven | TUE |
| Universiteit Gent | UG |
| Keysight Technologies | Keysight |
| Finisar Germany GmbH | Finisar |
| Orange SA | Orange |
| Technische Universitaet Berlin | TUB |
| Instituto Superior Tecnico, University of Lisboa | IST |

Abbreviations

| | |
|-------|-----------------------------------|
| GA: | Grant Agreement |
| GSNR: | Generalized Signal-to-Noise Ratio |
| SPM: | Self-Phase Modulation |
| XPM: | Cross-Phase Modulation |
| FWM: | Four-Wave-Mixing |
| NLI: | Non-linear Interference |
| WDM: | Wavelength-Division Multiplexed |
| QoT: | Quality of Transmission |
| ASE: | Amplified Spontaneous Emission |
| CUT: | Channel Under Test |
| SNR: | Signal-to-Noise Ratio |
| LP: | Light-path |
| PSD: | Power Spectral Density |
| SSFM: | Split-Step Fourier Method |
| P&P: | Pump-and-Probe |
| QPSK: | Quadrature Phase Shift Keying |
| EDFA: | Erbium-Doped Fiber Amplifier |
| CPE: | Carrier Phase Estimation |
| NLPN: | Non-linear Phase Noise |
| GN: | Gaussian Noise |
| OLS : | Optical Line System |

Contents

| | |
|--|----|
| LIST OF FIGURES | 5 |
| EXECUTIVE SUMMARY | 6 |
| 1. Overview of NLI Generation in Wideband Optical Networks..... | 7 |
| 2. Simulative Study on Spectral and Spatial Disaggregation | 9 |
| 3. Results and Analysis..... | 11 |
| 4. Conclusions..... | 13 |
| JUSTIFICATION OF DELAY | 14 |
| MITIGATION PLAN | 14 |
| REFERENCES | 15 |

LIST OF FIGURES

| | | |
|----------|---|------|
| Figure 1 | The normalized PSD observed before (blue) and after (red) propagation | p.9 |
| Figure 2 | (a) A diagram of the simulation workflow (b) an example constellation diagram of the QPSK modulated probe in a P&P simulation. | p.9 |
| Figure 3 | The error at the last span, ϵ_{20} , between all full-spectrum and superimposed P&P scenarios for Gaussian modulated input signals. | p.11 |
| Figure 4 | The SNR increments, ΔSNR for the P&P superpositions for both Gaussian modulated input signals and those without predistortion, the SPM, and an XPM accumulation analytically derived from the GN model. | p.12 |
| Figure 5 | A configuration scenario where the SPM is seen to be the main contributor to the SNR increment (in this case, after as few as 6 spans). | p.12 |

EXECUTIVE SUMMARY

The present scientific deliverable is part of the Work Package 1 “Network management: planning and control”, in turn part of the ETN project WON “Wideband Optical Networks”, funded under the Horizon 2020 Marie Skłodowska-Curie scheme Grant Agreement 814276.

This document provides details upon the derivation and simulative assessment of a spatially and spectrally disaggregated model for Non-linear Interference (NLI) generation within optical networks. Within this model the Self-Phase Modulation (SPM) and Cross-Phase Modulation (XPM) contributions are considered independently and on a channel-by-channel and span-by-span basis, taking into account the coherent accumulation effect of the SPM and allowing the Signal-to-Noise Ratio (SNR) accumulation of arbitrary spectral configurations to be calculated. This model is verified via an extensive simulation campaign that encompasses a wide range of fiber dispersion values, symbol rates, and Wavelength-Division Multiplexed (WDM) grid spacings. We remark that this approach remains valid for wideband transmission scenarios, such as for ITU-T G.652D-type fiber transmitting over the L+C+S+E and partial O bands, for fiber span lengths of tens of kilometers. We conclude that modelling the generation of NLI for wideband, disaggregated, and high-symbol rate transmission scenarios is possible using the presented approach.

1. Overview of NLI Generation in Wideband Optical Networks

The common quantifier for Quality of Transmission (QoT) degradation in optical networks deploying coherent technology is the Generalized Signal-to-Noise Ratio (GSNR) [1], given by

$$\text{GSNR} = (\text{OSNR}^{-1} + \text{SNR}_{\text{NL}}^{-1})^{-1}$$

The GSNR accounts for two principal effects: the NLI generated due to nonlinear transmission through the fiber medium (SNR_{NL}) and the Amplified Spontaneous Emission (ASE) noise that arises from optical amplification (OSNR). Adequately modelling these two contributions is essential in attaining the highest possible QoT, which is a requirement for enabling the maximum possible network throughput and bandwidth. Considering first the ASE noise, this is a linear effect that can either be predicted through characterization of the deployed amplifiers or more robust techniques such as machine learning [2]. On the other hand, the NLI is a coherent effect [3-5] with three main contributors: the SPM, XPM and Four-Wave-Mixing (FWM), with the latter shown to be negligible for a wide range of transmission scenarios [6-8].

The coherency of the NLI implies that its generation in fiber spans is dependent upon the NLI generated in previously crossed fiber spans, preventing its quantification in a scenario that is completely agnostic with respect to the network configuration. The XPM and SPM effects have been shown to be separable [4,6,7] for a wide range of use cases [9], with the former accumulating incoherently and the latter entirely providing the coherent contribution to the total NLI. This contribution can be quantified by considering its asymptotic accumulation and enforcing an upper bound [8].

First considering spectral disaggregation, the NLI power generated for a given CUT in an arbitrary spectral configuration, P_{NLI} , may be expressed as a sum of all individual contributions for each channel of index k :

$$P_{\text{NLI}} = \underbrace{P_{\text{NLI},0}}_{\text{SPM}} + \underbrace{\sum_{k \neq 0} P_{\text{NLI},k}}_{\text{XPM}}$$

Next, considering spatial disaggregation, $P_{\text{NLI},k}$ may be expressed in terms of the contribution of each fiber span n as:

$$P_{\text{NLI},k} = \sum_n^{N_s} P_{\text{NLI},k,n} = N_s \int_{\Omega_s} \frac{d\omega}{2\pi} \mathcal{G}_k(\omega)$$

where N_s is the total number of fiber spans, $\Omega_s = R_s/2\pi$ where R_s is the baud rate and $\mathcal{G}_k(\omega)$ is the PSD of the NLI generated in the k th channel. Assuming a worst-case transmission scenario where all input signals are stochastic Gaussian processes, it is possible to write the Power Spectral Density (PSD) for the NLI across the entire bandwidth for a single span through the first order non-linear

solution of the Manakov equation (it has been demonstrated that the polarization mode dispersion (PMD) has a negligible interaction with NLI generation [10]):

$$\begin{aligned} \partial_z \hat{N}_{0,x,y}(z, \omega) = & -i\gamma \left(\frac{8}{9} \right) e^{-2\alpha z} \iint_{-\infty}^{\infty} \frac{d\omega_1}{2\pi} \frac{d\omega_2}{2\pi} e^{-\frac{i}{2}\beta_2[\omega_1^2 - (\omega_1 - \omega_2)^2 + (\omega - \omega_2)^2 - \omega^2]} z \times \\ & \times \{ [\hat{E}_k(\omega_1) \cdot \hat{E}_k^*(\omega_1 - \omega_2)] \hat{E}_{0,x,y}(\omega - \omega_2) + [\hat{E}_0(\omega_1) \cdot \hat{E}_k^*(\omega_1 - \omega_2)] \hat{E}_{k,x,y}(\omega - \omega_2) \} \end{aligned}$$

where γ and α are the fiber non-linear coefficient and attenuation, respectively. If one assumes that the channel distribution remains the same throughout all fiber spans, it is possible to recover the PSD for the total XPM effect:

$$\begin{aligned} \mathcal{G}_k(\omega) &= \mathcal{F}^{-1} [\langle N^*(z, t) \cdot N(z, t + \tau) \rangle] = \\ &= 2\gamma^2 \left(\frac{8}{9} \right)^2 \left\{ \left[2 \left(\langle |\rho_{x,k}|^4 \rangle - \langle |\rho_{x,k}|^2 \rangle^2 \right) + \left(\langle |\rho_{y,k}|^4 \rangle - \langle |\rho_{y,k}|^2 \rangle^2 \right) \right] \langle |\rho_{x,0}|^2 \rangle + \right. \\ &\quad \left. + \langle |\rho_{y,0}|^2 \rangle \langle |\rho_{y,k}|^2 \rangle \langle |\rho_{y,k}|^2 \rangle \right\} \left(\frac{2\pi}{\Omega_s} \right)^3 \iint_{-\infty}^{\infty} \frac{d\omega_1}{2\pi} \frac{d\omega_2}{2\pi} I_k(\omega_1) I_k(\omega_1 - \omega_2) I_0(\omega - \omega_2) L^2(\omega; \omega_1, \omega_2) = \\ &= \frac{4\pi\gamma^2}{\Omega_s^3} \frac{64}{81} \{ 2P_{k,x}^2 P_{0,x} + P_{k,y}^2 P_{0,x} + P_{0,x} P_{k,y} P_{k,x} \} \iint_{-\infty}^{\infty} d\omega_1 d\omega_2 I_k(\omega_1) I_k(\omega_1 - \omega_2) I_0(\omega - \omega_2) L^2(\omega; \omega_1, \omega_2) \end{aligned}$$

where the $\langle \dots \rangle$ operator is the expectation value over all possible realizations of the given stochastic process, $I_{0,k}$ are the characteristic functions of the pump and probe bandwidths and L given by

From this standpoint it is possible to formulate a model which considers both spectral and spatial disaggregation, allowing the NLI contributions to be summed on a span-by-span and channel-by-channel basis. Subsequently, the SNR of each channel to be calculated, considering the accumulation of the SPM and XPM separately on a span-by-span basis, is given by:

$$\text{SNR}_{\text{NL}} = \left[\sum_{n=1}^{N_s} \left(\frac{1}{\text{SNR}_{\text{NL},n,0}} + \sum_{k \neq 0} \frac{1}{\text{SNR}_{\text{NL},n,k}} \right) \right]^{-1}$$

We highlight that, if this model allows the NLI generation to be successfully predicted, it will enable highly or fully disaggregated optical networks to be modelled without significant inaccuracies that arise from aggregated and incoherent models. It specifically applies to cases where the spectral configuration must be considered on a channel-by-channel basis, such as for alien wavelengths, or for fiber spans under the operation of different optical line system controllers. This would allow each channel and each fiber span to be considered on an individual basis. This motivates an investigation on the validity and accuracy of this model. Thus, we conducted an extensive simulation campaign for a wide range of transmission and fiber configuration scenarios.

2. Simulative Study on Spectral and Spatial Disaggregation

To investigate the spectral and spatial disaggregation hypotheses, we compared two distinct simulation scenarios through an extensive split-step Fourier method (SSFM) simulation campaign using an internally developed MATLAB® based software framework [11]. Scenario (1), referred to as *full-spectrum* simulation, represents a multi-channel WDM signal that aims to capture all propagation effects. Scenario (2), denoted to as the *superimposed* simulation, instead is a subset of many individual pump-and-probe (P&P) simulations that constitute the full-spectrum scenario, aiming to capture solely the XPM contributions. By additionally running the corresponding single-channel SPM simulations, a superposition of all P&P simulations may be produced for comparison with the full-spectrum case. An example of normalized PSD after propagation through 20 spans is shown in Fig. 1 for scenarios (1) and (2), respectively, using the simulation setup presented in Fig. 2.

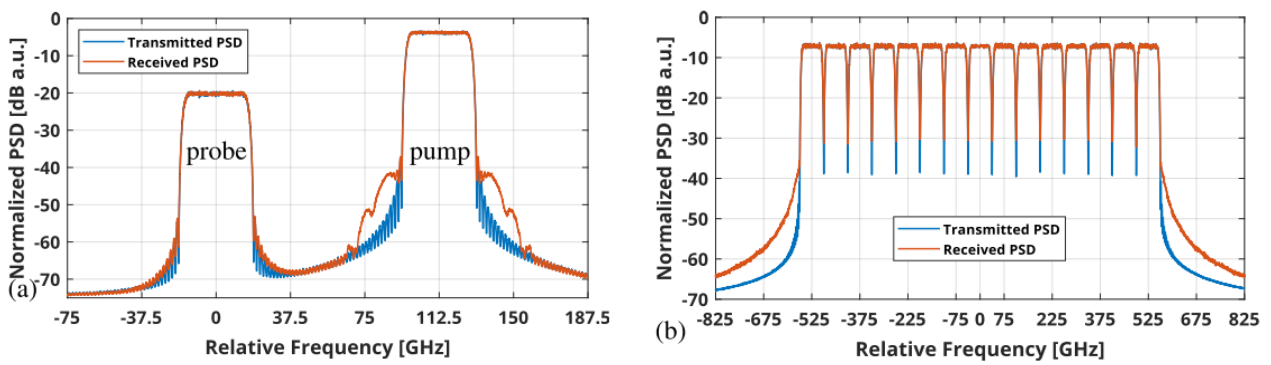


Figure 1: The normalized PSD observed before (blue) and after (red) propagation for (a) a P&P simulation and (b) a full-spectrum simulation.

The simulation set-up shown in Fig. 2 consists of an Optical Line System (OLS) with 20 fiber spans, each 80 km long for three different chromatic dispersion coefficient values: $D = 16.7, 5$ and 2 ps/(nm·km). These chromatic dispersion values refer to typical chromatic dispersion of standard single mode fiber (SSMF) in transmission bands ranging from L to E, and part of the O band. At the end of each span, an ideal, flat and noiseless Erbium-Doped Fiber Amplifier (EDFA) is used to compensate the propagation loss. The software simulates a dense WDM comb signal originating from a DSP-based coherent transceiver with a QPSK modulated CUT. After the 20 spans, the signal is processed by a carrier phase estimation (CPE) stage that utilizes the Viterbi-Viterbi algorithm [12], allowing full recovery of the nonlinear phase noise (NLPN).

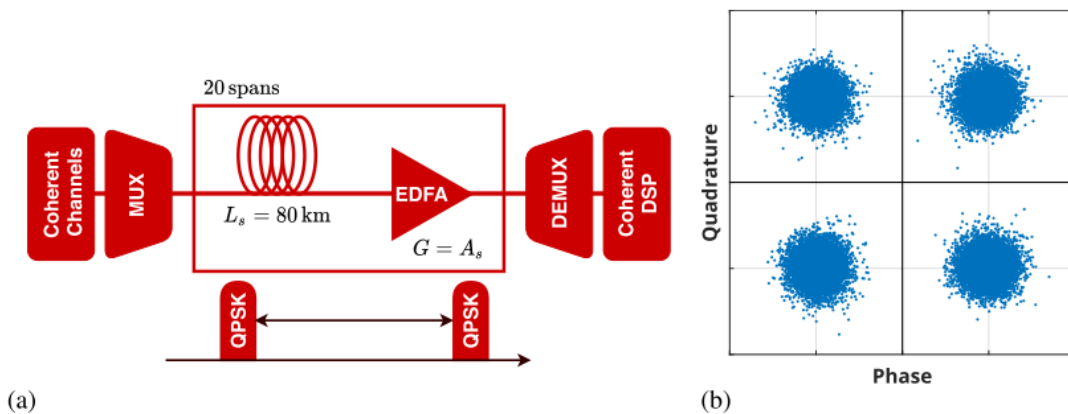


Figure 2: (a) A diagram of the simulation workflow, (b) an example constellation diagram of the QPSK modulated probe in a P&P simulation.

For all scenarios described, five pairs of symbol rates (R_s) and WDM grid spacings (Δf) shown in Table 1 are tested. The WDM comb has a width of approximately 1 THz, with the CUT always being the central channel of the comb. Concerning the launch power chosen in scenario (1), we use the local-optimization global-optimization (LOGO) power approach [13], calculated for each symbol rate/WDM grid combination. Regarding scenario (2), we set the probe power sufficiently low in order to isolate the XPM contribution: for a pump far from the probe signal we set the power to -20 dBm and for a pump close to the probe we set the LOGO power attenuated by 4 dB in order to mitigate the linear crosstalk of the pump on the probe.

Table 1: List of the different spectral configurations used in the simulation campaign. The third column shows the ratio between the symbol rate and WDM grid spacing.

| Symbol Rate (Gbaud) | WDM Grid Spacing (GHz) | Ratio | Num. channels |
|---------------------|------------------------|-------|---------------|
| 32 | 37.5 | 0.85 | 29 |
| 32 | 50 | 0.64 | 21 |
| 42.5 | 50 | 0.85 | 21 |
| 64 | 72 | 0.85 | 15 |
| 85 | 100 | 0.85 | 11 |

3. Results and Analysis

Firstly, to test the extent of the spectral disaggregation hypothesis, the error ϵ_n in SNR at span n between the accumulations of the full-spectrum $SNR_{Full,n}$ and the accumulations of the P&P superposition was evaluated using:

$$\epsilon_n = SNR_{Full,n} - SNR_{Sup,n}$$

Fig. 3 shows ϵ_{20} , i.e., the error between the full-spectrum and superimposed P&P scenarios after transmission along 20 fiber spans. Results indicate that the full-spectrum result can be estimated from a P&P superposition within a 0.5 dB degree of accuracy, hence demonstrating the potential of the spectral disaggregation approach to calculate the SNR, even for the worst case scenarios considered within this simulation campaign.

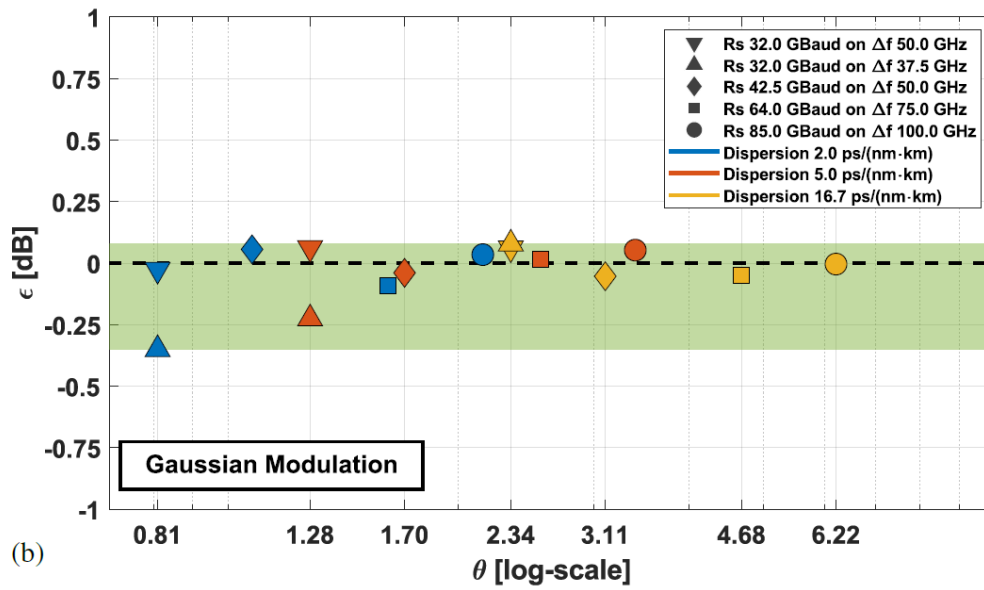


Figure. 3. Error in the estimation of the SNR after 20 fiber spans transmission, ϵ_{20} , between full-spectrum and superimposed P&P scenarios for Gaussian modulated input signals.

Considering next the prospect of spatial disaggregation, the span-by-span NLI degradation is considered by taking the SNR contribution, ΔSNR , presented in dB. A selection of these results for the wideband dispersion case (when chromatic dispersion may attain $D = 2$ ps/(nm·km)) is presented in Fig. 4, considering superpositions for both Gaussian modulated input signals and those without predistortion.

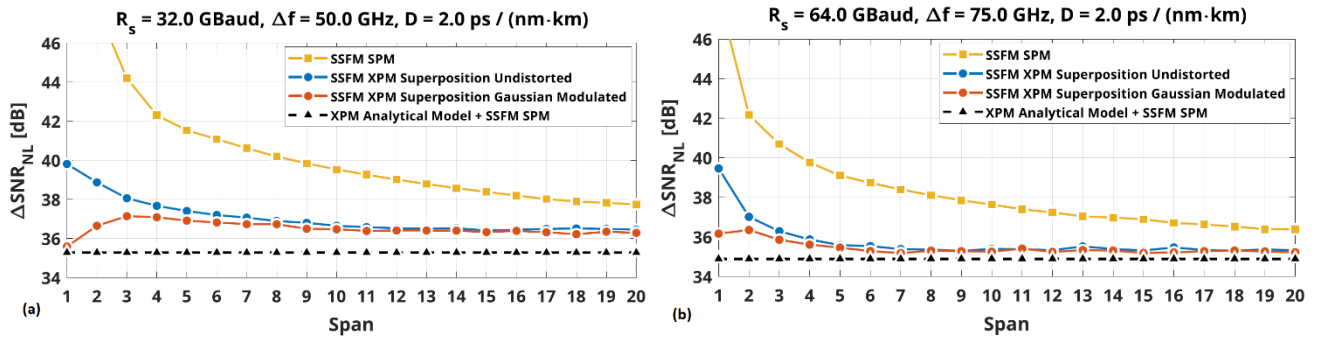
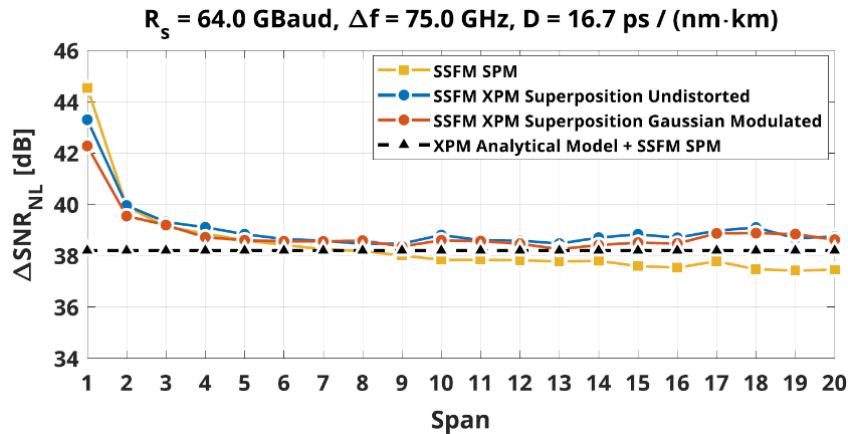


Figure 4. The span-by-span SNR decrease (ΔSNR) in dB for a variety of simulations. The blue and red lines are the P&P superpositions for transmission cases without predistortion and for Gaussian modulation. The yellow line is the considers single channel NLI only (SPM), obtained from a single-channel simulation. In black, we present the effect of XPM accumulation analytically derived from the disaggregated GN model [4].

Fig. 4 (a) and (b) clearly show that the nonlinear SNR contribution of each span due to the SPM NLI decreases with the span (larger SPM NLI contribution of each span) count demonstrating coherent accumulation, whereas the contribution caused by XPM NLI is approximately independent of the span count after transmission along just a very short number of transient spans: It indicates an incoherent accumulation behaviour, i.e., the same amount of XPM NLI introduced by each fibre span. This behaviour was found for all configurations in the simulation campaign, demonstrating spatial disaggregation for a wide range of scenarios. Furthermore, instances where the SPM is the dominant contribution to the NLI accumulation were also found, such as the one highlighted in Fig. 5, further reinforcing the need for a coherent NLI model when considering wideband, disaggregated, and high



symbol rate transmission scenarios.

Figure 5. Scenario where the SPM is the main contributor to the SNR decrement (after as few as 6 spans).

4. Conclusions

Within this work, we present the derivation of a NLI model which considers the XPM and SPM within a fully separable, spectrally and spatially disaggregated standpoint. We conducted an extensive SSFM simulation campaign, including dispersion cases representative of E, L and partial O-band transmission, demonstrating that this model can be applied with a high level of accuracy. We additionally demonstrate that, in specific cases, SPM becomes the main contributor to the generation of NLI, requiring a coherent model, such as the one presented here, to be considered to retain accurate SNR estimations.

We wish to further highlight that the results and approaches presented within this work are summaries that contain only a subset of obtained results. Additional details can be found in our other recent publications [2, 5, 14, 15] and a previous work [4] which explains these conclusions in greater detail.

JUSTIFICATION OF DELAY

The original submission date for this work package was specified to be June 2020. However, the complete submission of this work package was delayed until December 2020 because of unforeseen circumstances. In early March 2020, the POLITO and all other consortium membership institutions were forced to temporarily close for an extended period because of the COVID-19 pandemic. This work package was negatively affected by these sudden quarantine measures, with the lockdown only beginning to ease in mid-June 2020, but with the POLITO remaining fully closed until October 2020. Consequently, all POLITO staff adapted to new smart-working procedure that had to be implemented at short notice, which caused significant coordination and technical issues which had to be overcome – with all contributors to this work package being affected by being unable to directly access their primary workstations.

MITIGATION PLAN

As a result of the aforementioned delays, mitigation actions were put into place. Firstly, all contributors to this work package were able to adapt to smart-working procedures after an initial troubleshooting period that coincided with the initial implementation of the quarantine, with no further delays being anticipated. The POLITO contributors to this work package are now fully prepared in case of further COVID-19 disruptions, with an effective smart-working regime now being implemented.

The international quarantine imposed due to COVID-19 has caused a similar degree of disruption to all other work packages and, as a result, a 6-month extension has been implemented for the main project timeline. We evaluate that the delay of this project will therefore impart minimal impact upon other dependent deliverables within this work package (D1.2 and D1.3) and future work hosted at this institution will progress as originally planned.

REFERENCES

- [1] Filer, M., Cantono, M., Ferrari, A., Grammel, G., Galimberti, G. and Curri, V., 2018. Multi-vendor experimental validation of an open source QoT estimator for optical networks. *Journal of Lightwave Technology*, 36(15), pp.3073-3082.
- [2] D'Amico, A., Straullu, S., Nespola, A., Khan, I., London, E., Virgillito, E., Piciaccia, S., Tanzi, A., Galimberti, G. and Curri, V., 2020. Using machine learning in an open optical line system controller. *Journal of Optical Communications and Networking*, 12(6), pp.C1-C11.
- [3] Dar, R., Feder, M., Mecozzi, A. and Shtaif, M., 2013. Properties of nonlinear noise in long, dispersion-uncompensated fiber links. *Optics Express*, 21(22), pp.25685-25699.
- [4] Virgillito, E., D'Amico, A., Ferrari, A. and Curri, V., 2019, July. Observing and Modeling Wideband Generation of Non-Linear Interference. In *2019 21st International Conference on Transparent Optical Networks (ICTON)* (pp. 1-4). IEEE.
- [5] D'Amico, E. London, E. Virgillito, A. Napoli, and V. Curri, "Quality of transmission estimation for planning of disaggregated optical networks," in *2020 International Conference on Optical Network Design and Modeling (ONDM)*, (2020), pp. 1–3.
- [6] Miao, X., Bi, M., He, H. and Hu, W., 2017, July. Four-wave mixing effect reduction in O-band multi-wavelength NG-EPON system based on chirped DML. In *2017 Opto-Electronics and Communications Conference (OECC) and Photonics Global Conference (PGC)* (pp. 1-3). IEEE.
- [7] Carena, A., Bosco, G., Curri, V., Jiang, Y., Poggiolini, P. and Forghieri, F., 2014. EGN model of non-linear fiber propagation. *Optics express*, 22(13), pp.16335-16362.
- [8] Carena, A., Bosco, G., Curri, V., Poggiolini, P. and Forghieri, F., 2013, September. Impact of the transmitted signal initial dispersion transient on the accuracy of the GN-model of non-linear propagation. In *39th European Conference and Exhibition on Optical Communication (ECOC 2013)* (pp. 1-3). IET.
- [9] Johannisson, P. and Karlsson, M., 2013. Perturbation analysis of nonlinear propagation in a strongly dispersive optical communication system. *Journal of Lightwave Technology*, 31(8), pp.1273-1282.
- [10] Cantono, M., Piori, D., Ferrari, A., Carena, A. and Curri, V., 2018, March. Observing the interaction of PMD with generation of NLI in uncompensated amplified optical links. In *2018 Optical Fiber Communications Conference and Exposition (OFC)* (pp. 1-3). IEEE.
- [11] Piori, D., Bertignono, L., Nespola, A., Forghieri, F. and Bosco, G., 2017. Comparison of probabilistically shaped 64QAM with lower cardinality uniform constellations in long-haul optical systems. *Journal of Lightwave Technology*, 36(2), pp.501-509.
- [12] Viterbi, A., 1983. Nonlinear estimation of PSK-modulated carrier phase with application to burst digital transmission. *IEEE Transactions on Information theory*, 29(4), pp.543-551.
- [13] Pastorelli, R., Piciaccia, S., Galimberti, G., Self, E., Brunella, M., Calabretta, G., Forghieri, F., Siracusa, D., Zanardi, A., Salvadori, E. and Bosco, G., 2013, September. Optical control plane based on an analytical model of non-linear transmission effects in a self-optimized network. In *39th European Conference and Exhibition on Optical Communication (ECOC 2013)* (pp. 1-3). IET.

- [14] E. London, E. Virgillito, A. D'Amico, A. Napoli, and V. Curri, "Simulative assessment of non-linear interference generation within disaggregated optical line systems," *OSA Continuum Vol. 3*, 3378-3389 (2020).
- [15] E. London, E. Virgillito, A. D'Amico, A. Napoli and V. Curri, 2020. "Analysis of the Coherent Contributions to Nonlinear Interference Generation within Disaggregated Optical Line Systems", *arXiv preprint arXiv:2012.01896*.